Sensors and Actuators A 264 (2017) 51–57

Contents lists available at ScienceDirect

Sensors and Actuators A: Physical

journal homepage: www.elsevier.com/locate/sna

Understanding the effect of carbon in carbon/salt/adhesive electrodes for surface electromyography measurements

Hugo F. Posada-Quintero [a], Ryan Rood [a], Ken Burnham [b], John Pennace [b], Ki H. Chon [a,*]

[a] University of Connecticut, Storrs, CT 06269 USA
[b] FLEXcon, Spencer, MA 01562 USA

ARTICLE INFO

Article history:
Received 18 April 2017
Received in revised form 20 June 2017
Accepted 31 July 2017
Available online 1 August 2017

Keywords:
Salt/adhesive electrodes
Carbon/salt/adhesive electrodes
Dry electrodes
Surface electromyography

ABSTRACT

Dry electrodes that do not require silver and hydrogel might provide the advantages of having very long shelf life and lower cost, compared to the gold standard Ag/AgCl hydrogel electrodes. Recently, we compared novel carbon/salt/adhesive (CSA) electrodes with Ag/AgCl electrodes for surface electromyography (sEMG) signal collection. We found no significant differences in amplitude, but CSA electrodes outperformed Ag/AgCl in response to noise and motion artifacts. However, the carbon component may be redundant, and the salt/adhesive (SA) mixture might be as effective as CSA for such a task. In the SA electrodes, the salt concentration is the only tunable factor. To determine if carbon contribution is necessary for effective sEMG measuring capabilities, we varied the salt concentration in the SA electrodes to 10%, 15%, and 25% and their performance was compared to the functional capabilities of CSA electrodes. Twenty subjects were recruited to collect simultaneous recordings of sEMG signals using CSA and SA electrodes, side-by-side on triceps brachii, tibial anterior muscles, biceps brachii and quadriceps femoris. SA 15% and SA 25% electrodes detected higher amplitude values during contraction in biceps, tibials and quadriceps, compared to CSA. All SA electrodes exhibited high mean correlation with CSA electrodes, on the linear envelopes ($\geq$ 0.887), RMS envelope ($\geq$ 0.87) and power spectrum density ($\geq$ 0.94). SA 15% and SA 25% electrodes performed better in response to noise and were more sensitive to myoelectric activity than CSA electrodes, but CSA electrodes exhibited better response to motion artifacts than SA electrodes. SA 10% electrodes presented high electrode-skin impedance, producing some lower values in sEMG signals during contraction, worse motion corruption and spectral deformation compared to CSA. Results suggest that carbon improves capability to manage motion, but at the expense of more susceptibility to noise corruption. Higher salt concentration reduced motion artifacts and spectral deformation, but reduced the sensitivity to myoelectric signals. In conclusion, SA electrodes, specifically the mixture with 15% salt, provided a better response to myoelectric activity and seem to be the most suitable alternative for sEMG data collection.

1. Introduction

Novel dry electrodes designed by combining carbon black powder with a quaternary salt and visco-elastic polymeric adhesive [1] (termed carbon/salt/adhesive or CSA electrodes) were recently compared for their functional performance to the standard Ag/AgCl electrode when acquiring surface electrocardiographic (sEMG) signals [2]. It was found that CSA electrodes outperformed Ag/AgCl electrodes for sEMG data collection. Hence, any new electrode design for sEMG applications should be benchmarked against CSA electrodes.

CSA electrodes consist of three components: the conductive layer, the adhesive layer and the bridge [3]. The adhesive layer contains the carbon/salt/adhesive mixture. To reduce the impedance, carbon particles of this layer are aligned in the Z direction through the activation (electrophoresis) process. The third component, the bridge, is needed in order to connect the isolated Z direction conductive pathways.

Although CSA electrodes have been shown to be a suitable surrogate for Ag/AgCl electrodes for sEMG, further investigation needs to be performed to better understand the contribution of carbon as a conductive material for sEMG data collection. If carbon is found to be unnecessary, the activation process and the bridge are also unnecessary, making the fabrication process easier, leading to potentially less expensive electrodes. The precursor to CSA electrodes is a signal receptive material that did not contain carbon for its fabrication (a mixture of salt and adhesive, SA). This type of

* Corresponding author.
E-mail address: kchon@engr.uconn.edu (K.H. Chon).

http://dx.doi.org/10.1016/j.sna.2017.07.055
0924-4247/

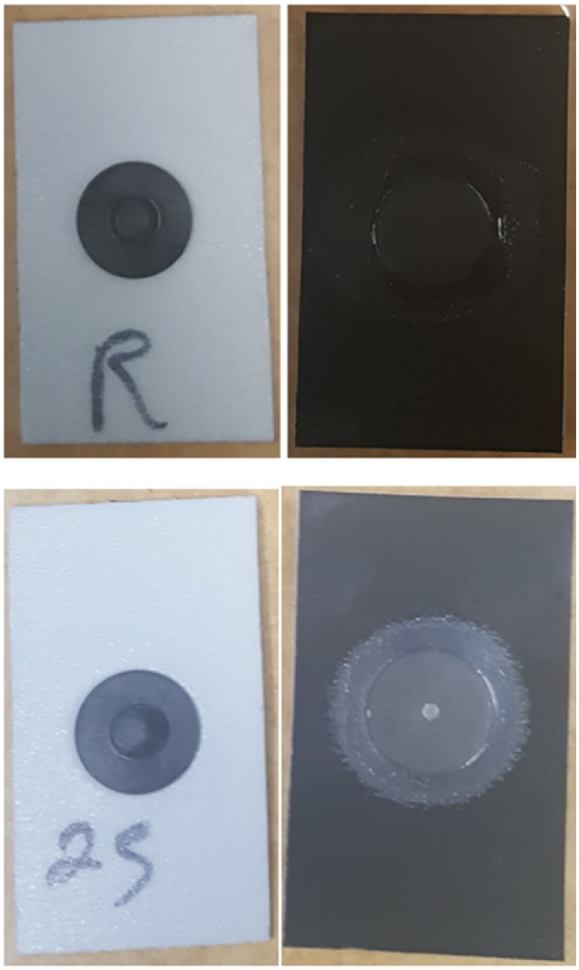

Fig. 1. Connector and contact side of tested sEMG electrodes. Top: CSA electrodes (the label R in the plot means "Reference"); bottom: SA electrodes (25% salt). Dimensions are 1 1/2" x 7/8" (3.81 cm x 2.22 cm) for both.

electrode was not tested for collection of sEMG signals. CSA and SA electrodes look similar because the conductive layer is still carbon for both, and the bridge layer coincides with the bottom part of the snap connector (Fig. 1).

As salt is conductive, the elimination of carbon can be compensated for by increasing the salt concentration of the adhesive layer. To determine the optimal salt concentration, the SA electrodes were tested with three different levels (10%, 15%, and 25%) and they were each compared to the CSA electrodes. These different concentrations will determine whether the carbon contribution is a necessary ingredient for effective sEMG measuring capabilities of CSA electrodes, and if salt alone (at the optimal concentration) can provide similar functional performance to that of CSA electrodes.

2. Materials and methods

2.1. Electrode fabrication

The CSA sEMG electrodes' fabrication process has been described before [2–4]. Succinctly, to create CSA-based sEMG electrodes, the conductive base layer, the adhesive, and the bridge are prepared beforehand. The conductive layer is made with a polyethylene foam carrier coated with an electrically conductive material consisting of a polymeric binder loaded with conductive fillers. The adhesive layer is a releasable carrier coated with a doped adhesive such as an acrylic pressure sensitive type loaded with conductive carbon filler and a quaternary ammonium salt. The salt in the mixture does not have any significant disassociation. It does not separate into ions as would be the case for NaCl in water, for example. The adhesive layer of CSA electrodes used in this study contain 15% salt. The adhesive layer of CSA electrodes requires an activation process through electrophoresis. The bridge is a conductivity-enhancing conduit made of low impedance electrically conductive material that produces a lower electrode ohm value by connecting in parallel multiple isolated Z direction (out of plane) conductive pathways in the adhesive layer.

Fabrication of SA electrodes requires only the conductive layer and the adhesive. In this case, the adhesive is loaded only with quaternary ammonium salt. Thus, SA electrodes require neither carbon in the adhesive layer, nor the activation process nor the bridge feature. CSA and SA electrodes' dimensions are 1 1/2" x 7/8" (3.81 cm x 2.22 cm).

2.2. Electrode-skin contact impedance measurements

Electrode-skin impedance measurements were carried out using CSA and SA electrodes. The skin of the test subject was cleaned before each measurement by wiping with a 2%-alcohol impregnated cotton pad, which was allowed to evaporate before applying the electrodes. Two identical (CSA or SA) electrodes were mounted on the left forearm, one on the palm side of the wrist, and the second 5 cm apart from the first but situated towards the elbow. These electrodes were connected to a Hioki IM3570 impedance analyzer, and each measurement was the result of averaging 20 measurements. The signal voltage amplitude was set to 1 V and the frequency range varied from 4 to 2 KHz. N = 8 electrodes of each type of electrode were used (CSA, SA 10%, SA 15%, SA 25%). To keep skin properties as constant as possible, all measurements were performed in a single day.

2.3. Protocol for sEMG signal collection

The protocol was similar to that used in a previous study [2]. The procedure described below was repeated three times on each subject taking part in the experiment, since we wanted to try three levels of salt concentration in the SA electrodes (10%, 15%, and 25% salt concentration). To ensure accurate comparison between the electrodes, simultaneous measurements were recorded. To do this, SA and CSA electrodes were placed side-by-side. CSA and SA electrodes were placed on a lateral position (left or right on the same muscle) that alternated from subject to subject, to eliminate any bias from being only on one side.

sEMG signals were acquired using a Dual Bio Amp (ADInstruments) and digitized at a sampling frequency of 2 kHz. sEMG measurements of the biceps brachii, triceps brachii (long head), tibialis anterior, and quadriceps femoris (rectus femoris) were recorded in four separate parts of the experiment. The sampling frequency was selected to meet the requirements set in previous studies on sEMG that involved the muscles tested in this work [5–7]. The required sampling frequency is especially high for the biceps brachii and the tibials anterior. The same time frame was followed for sEMG signal recording on every muscle (Fig. 2). Subjects practiced the maneuvers prior to every test until they felt comfortable with the procedure.

We had subjects lift a weight of 3 lbs. (1.36 kg) for testing electrodes on triceps brachii and tibialis anterior muscles. For biceps brachii and quadriceps femoris, subjects used a weight of 6 lbs. (2.72 kg). Fig. 3 shows the areas where the electrodes were placed on each muscle [8]. The electrodes were placed with the subjects in the resting condition. sEMG measurements of the four muscles were recorded while subjects performed four muscle contraction maneuvers during the experiment, one for each muscle. These spe-

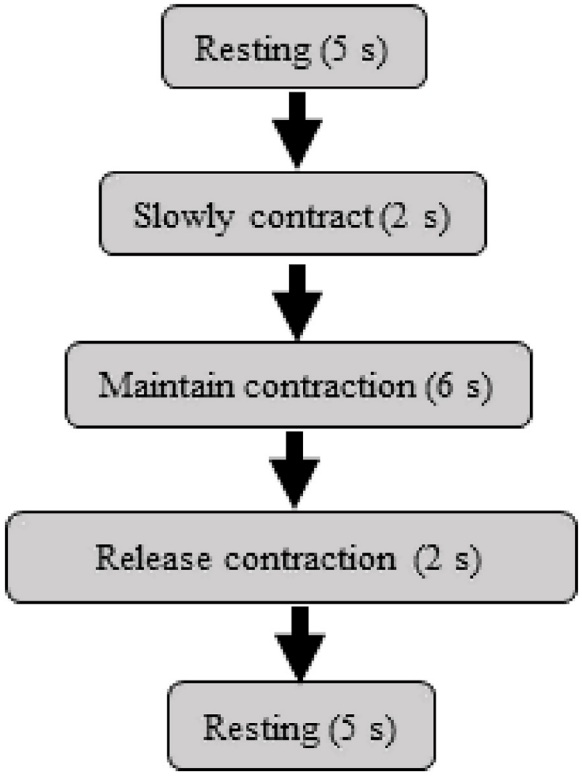

Fig. 2. Timeframe for movements while recording sEMG signal.

cific muscles were chosen based on their variance in size. It has been observed that muscles of varying sizes will produce sEMG signals of varying amplitudes.

Before performing every test, it was assured that the location where the electrodes were placed was hairless and had been wiped with alcohol and allowed to dry. As we took three recordings (one for each salt level), we removed the prior SA electrodes, prepared the site of the skin they were placed on, let it dry, and placed the next salt concentration level SA electrodes. The CSA electrodes remained in place for all three data recordings.

Subjects were asked to perform the following maneuvers: 1) contract their biceps, bringing the elbow to a 90° angle, with the forearm in supination; 2) contract their triceps and extend their elbow joint so that the weight was suspended backwards; 3) contract their tibialis anterior muscle and lift the weight off the floor without extension of the great toe; and 4) lift their leg up (extend their knee) to procure contraction of the quadriceps. The protocol was approved by the Institutional Review Board of the University of Connecticut.

2.4. Signal processing

We processed sEMG signals offline to quantify their quality and to compare the performance of SA electrodes (the three salt levels) to the CSA electrodes. First, the correlation between CSA and SA electrodes was computed in the time and frequency domains to test interchangeability between the two media, for the task of sEMG signal collection. Furthermore, several time- and frequency-domain indices of sEMG signals' quality were computed. The procedure to compute all indices is described below.

2.4.1. Time domain measures

2.4.1.1. a) Linear envelope. sEMG signals were rectified (by taking their absolute value), low-pass filtered at 10 Hz, and down-sampled to 41.66 Hz (a rate that is closer to motion frequencies) to get a linear envelope. The resulting envelope is an estimate of the standard deviation of the sEMG signal, which is in turn a measure of the muscles' power. The Pearson's correlation between CSA and Ag/AgCl electrodes' sEMG envelopes was computed, for each muscle, to test the similarity between the two simultaneously-acquired signals. Correlation provides an index of similarity, independent of the amplitude of the signals which were collected with the two types of electrodes side by side.

2.4.1.2. b) Amplitude. Mean value of the linear envelope was computed as an amplitude estimation of sEMG signals. This index was computed for relaxation and contraction stages, to evaluate the statistical differences in amplitudes between the signals obtained using CSA and Ag/AgCl electrodes.

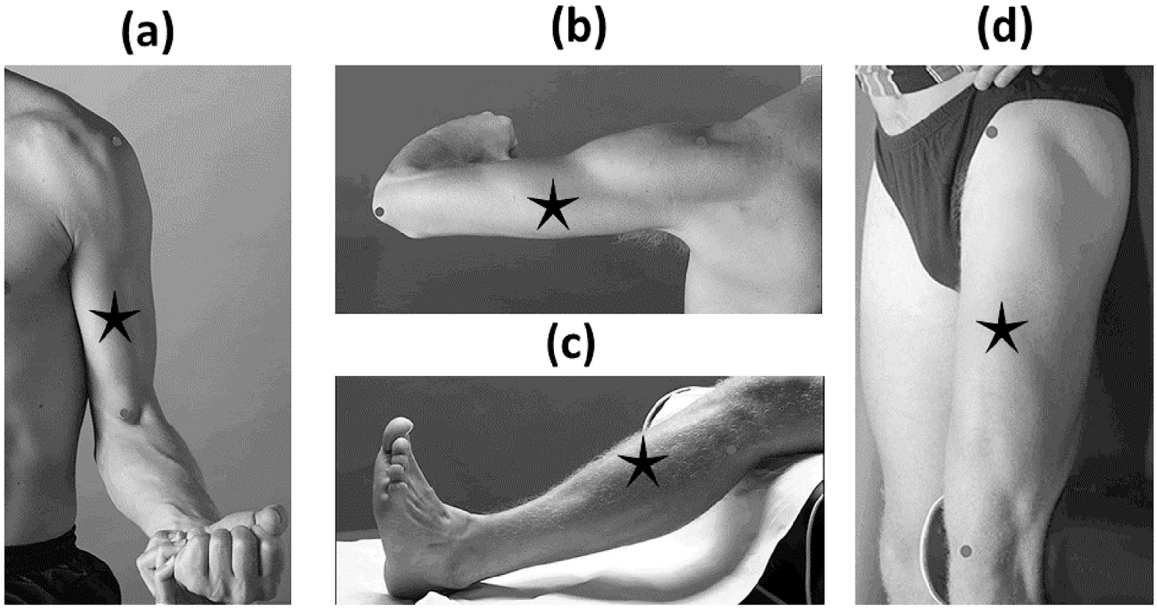

Fig. 3. Electrode placement. (a) biceps, (b) triceps, (c) tibials, (d) quadriceps. Star denotes the location of the electrodes on each muscle.

2.4.1.3. c) RMS envelope. The sEMG signals were divided into multiple windows of 25 ms [9]. RMS values were computed from the signals before rectification since the values have both negative and positive values. RMS values were calculated as follows:

$$RMS = \sqrt{\left(1/k_{max}\right) \cdot \sum_{k=0}^{k_{max}} signal_k^2}$$

where k_{max} is the number of samples in each 25 ms segment. As with the linear envelope, the Pearson's correlation between CSA and Ag/AgCl electrodes' sEMG RMS values were computed for each muscle.

2.4.2. Frequency domain measures

For frequency domain analysis, the power spectral density (PSD) of each sEMG signal was calculated using Welch's periodogram method with 50% data overlap. A Blackman window (length of 256 data points) was applied to each segment and the fast Fourier transform (FFT) was calculated for each windowed segment. Finally, the power spectra of the segments were averaged. An FFT segment size of 1024 data points was used.

2.4.2.1. a) PSD correlation. The raw sEMG data were used to perform frequency domain analysis. To test the similarity between CSA and Ag/AgCl sEMG signals in the frequency domain, the Pearson's correlation coefficient of PSD representations was computed.

2.4.2.2. b) SN Ratio. This index considers noisy disturbances in the high-frequency range of the PSD [10]. For the signal-to-noise (SN) ratio calculation, we assumed that noise had a constant power density over the frequency region of interest in sEMG recordings and that no muscular activity-related power was present above 800 Hz (upper 20% of the frequency range). Thus, first, the power for the frequency range above 800 Hz was calculated. The predicted total power of the noise is this power summed over the whole frequency range. The SN ratio was then calculated as the ratio of the total sEMG power to the total power of the noise.

2.4.2.3. c) SM Ratio. For this study, motion artifacts are defined as low-frequency fluctuations of the signal induced by mechanical alteration of the electrode-skin interface. Use of the signal-to-motion (SM) ratio is based mainly on two assumptions: 1) the frequency of motion-induced artifacts of the signal stay well below 20 Hz, and 2) the shape of the non-contaminated sEMG power spectrum is fairly linear between 0 and 20 Hz [11]. Consequently, the motion artifacts' spectral power will be mixed in with the true signal dynamics at frequencies between Hz. Per Sinderby et al. [11], the motion artifacts' power (grey area in Fig. 4) can be reasonably estimated by summing the PSD area below 20 Hz that exceeds a straight line between the origin and the highest mean power density. The highest mean power density (the red dot in the averaged spectral plot of Fig. 4) was defined as the largest mean spectral value within a window length of 25.4 Hz starting from 35 Hz to 500 Hz. Finally, the sum of the area under the PSD for all frequencies divided by the motion artifact power was computed to obtain the SM ratio.

2.4.2.4. d) DP ratio. The spectrum maximum-to-minimum drop in power (DP ratio) was obtained by computing the quotient between the highest and lowest mean PSD values. The mean PSD is obtained by averaging a spectral window length of 25.4 Hz (13 consecutive points). The DP ratio is an indicator of whether the spectral frequency contents of interest are adequately peaked, is sensitive to the signal's amplitude, and can detect the absence of sEMG activity. The DP ratio is not sensitive to power below 35 Hz (in contrast to the SN ratio) and will not provide falsely high values because of the power induced by motion artifacts. A higher DP ratio is desirable.

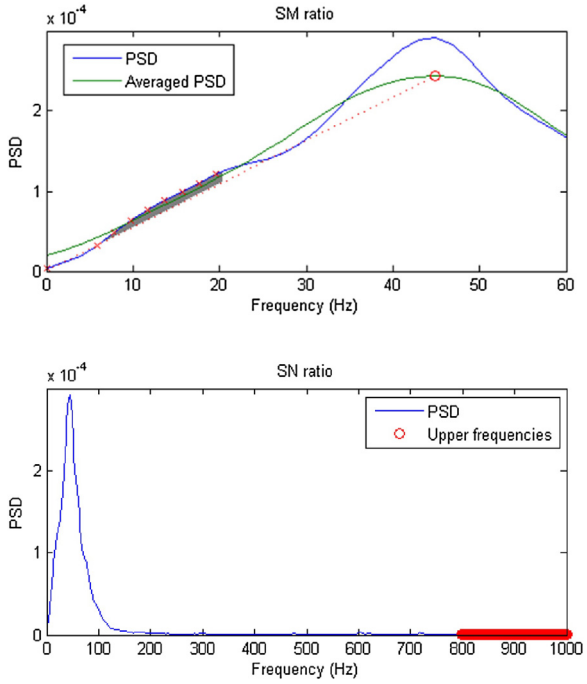

Fig. 4. Illustration of SM ratio (top) and SN ratio (bottom) estimation.

2.4.2.5. e) Ω ratio. The spectral deformation is computed in terms of spectral moments, as follows:

$$\Omega = \left(M_2/M_0\right)^{\frac{1}{2}} / \left(M_1/M_0\right),$$

where

$$M_n = \sum_{i=0}^{i_{max}} powerdensity_i \cdot frequency_i^n$$

Ω ratio is sensitive to changes in symmetry and peaking of the PSD and to additive disturbances in the high- and low-frequency regions [10]. This index identifies all dynamics of spectral changes except those caused by pure translations along the frequency axis. The feature is also sensitive to an excess of low-frequency power. A lower Ω is desirable.

The SN, SM and DP ratios are presented in decibels, and the Ω ratio is unitless. These four indices obtained for CSA and Ag/AgCl electrodes were compared for each muscle and in the overall, by testing for statistically significant differences, to examine whether there is an electrode media that collects the signal with lower noise power, lower motion-artifact corruption, more sensitivity to EMG activity, and lower distortion, respectively. This battery of indices have been used before to assess quality of myoelectric signals [2,12,13].

3. Results

Results for electrode-skin contact measurements are presented in Fig. 5. The impedance of SA electrodes is very sensitive to salt concentration. SA 10% electrodes exhibited the highest electrode-skin impedance, followed by SA 15%, CSA and SA 25%, throughout the range 4 Hz to 2 kHz. Representative sEMG signals acquired in the biceps of a given subject with SA 15% and CSA electrodes are shown in Fig. 6.

Table 1
Results for amplitude, envelope correlation and PSD correlation.

	Biceps		Triceps		Tibials		Quadriceps	
	Relaxation	Contraction	Relaxation	Contraction	Relaxation	Contraction	Relaxation	Contraction
Amplitude CSA	1.45 ± 1.11	10.6 ± 3.44	3.94 ± 2.4	23.8 ± 14.6	1.18 ± 0.34	10.7 ± 4.95	1.39 ± 0.94	16 ± 7.97
Amplitude SA 10%	1.83 ± 1.23*	12 ± 3.43*	4.29 ± 2.47	22.6 ± 14.1	1.92 ± 1.01*	9.99 ± 3.83	1.99 ± 1.46*	13.5 ± 5.24*
Amplitude CSA	1.57 ± 1.04	10.5 ± 3.36	3.48 ± 1.92	21.9 ± 15.2	1.44 ± 0.72	9.86 ± 4.1	1.16 ± 0.37	15.4 ± 7.68
Amplitude SA 15%	2.05 ± 1.24*	12.5 ± 3.64*	3.82 ± 1.91	21.8 ± 13.9	1.71 ± 0.51*	10.4 ± 4.96	1.45 ± 0.52*	15.2 ± 7
Amplitude CSA	1.7 ± 1.17	10.9 ± 3.17	3.61 ± 1.97	22.2 ± 10	1.19 ± 0.37	10.4 ± 5.14	1.12 ± 0.32	15.5 ± 7.24
Amplitude SA 25%	2.33 ± 1.56*	12.4 ± 3.26*	3.84 ± 2.09	22.5 ± 11.2	1.41 ± 0.3*	10.6 ± 5.59	1.41 ± 0.42*	15.8 ± 5.43
Correlation of linear envelope. SA vs. CSA electrodes								
SA 10%	0.88 ± 0.08		0.93 ± 0.04		0.87 ± 0.14		0.94 ± 0.04	
SA 15%	0.89 ± 0.05		0.93 ± 0.04		0.89 ± 0.13		0.95 ± 0.02	
SA 25%	0.89 ± 0.07		0.94 ± 0.03		0.93 ± 0.03		0.95 ± 0.02	
Correlation of RMS envelope. SA vs. CSA electrodes								
SA 10%	0.88 ± 0.07		0.93 ± 0.04		0.87 ± 0.14		0.94 ± 0.04	
SA 15%	0.89 ± 0.05		0.92 ± 0.04		0.88 ± 0.14		0.95 ± 0.01	
SA 25%	0.88 ± 0.07		0.94 ± 0.04		0.93 ± 0.03		0.95 ± 0.02	
Correlation of PSD. SA vs. CSA electrodes								
SA 10%	0.99 ± 0.01		0.97 ± 0.02		0.96 ± 0.07		0.94 ± 0.07	
SA 15%	0.99 ± 0.01		0.96 ± 0.04		0.98 ± 0.03		0.95 ± 0.04	
SA 25%	0.99 ± 0.01		0.97 ± 0.04		0.98 ± 0.01		0.94 ± 0.04	

Values are expressed as mean ± standard deviation.
Amplitude values are in mV.
CSA: carbon/salt/adhesive; SA: salt/adhesive; RMS: root mean square; PSD: power spectral density.

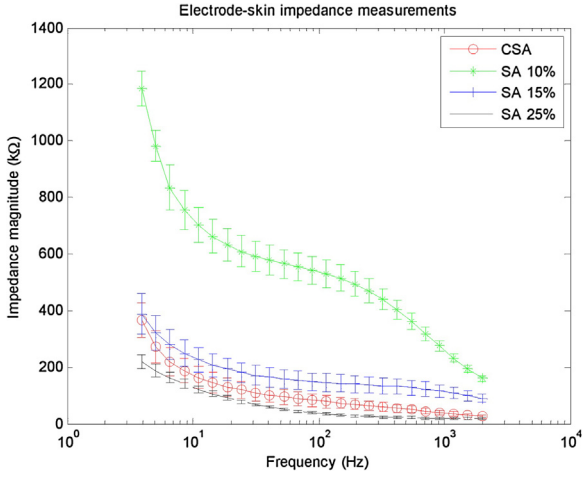

Fig. 5. Electrode-skin contact impedance measurements for CSA and SA electrodes.

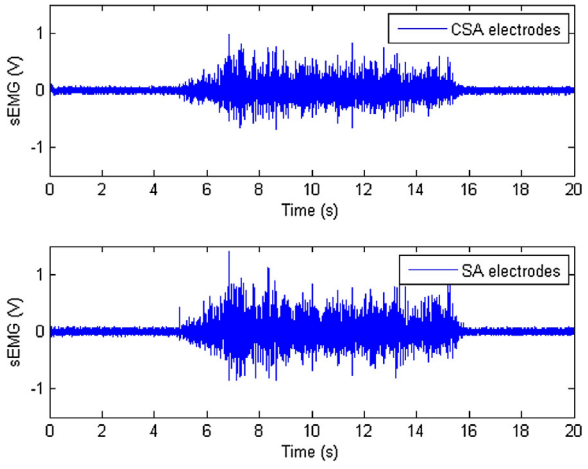

Fig. 6. Sample sEMG measures using CSA (top) and SA electrodes (bottom) on a given subject's biceps.

The results for amplitude, linear envelope, RMS envelope and PSD correlation are shown in Table 1. For all muscles, the amplitude of sEMG signals acquired using CSA and SA (10%, 15% and 25% salt) electrodes were higher on average during the contraction stage compared to the relaxation stage.

Some significant differences in amplitude measurements were found between CSA and SA sEMG signals. In the biceps, sEMG signals obtained using SA electrodes (any concentration) exhibited significantly higher amplitude compared to CSA electrodes, during both relaxation and contraction stages. The amplitude of sEMG measurements was also significantly higher for SA electrodes (any concentration) compared to CSA electrodes during the relaxation stage in tibials and quadriceps. No statistically significant differences were found in the sEMG measurements in the triceps.

The average correlation of linear envelope was equal to or higher than 0.87 between CSA and all three concentrations of SA electrodes. The correlation of RMS envelope was similar, as any average value was equal to or higher than 0.87. The correlation of spectra measured by PSD was very high, as mean values were equal to or above 0.94.

Table 2 includes the indices based on spectral analysis for quality assessment of sEMG signals. In general, the SN ratio was higher for SA electrodes. The SN ratio was significantly higher for all concentrations of SA electrodes in the biceps and for SA 15% in the quadriceps, compared to CSA electrodes. Measurements of SN ratio were not significantly different between CSA and SA electrodes in other cases.

Comparing values of the SM ratio of SA to CSA electrodes, the latter shower higher values overall. SA 10% showed significantly lower values in the triceps, tibials and quadriceps, SA 15% showed significantly lower values in the tibials and quadriceps, and SA 25% was significantly lower only in the quadriceps.

A higher salt concentration produced lower mean DP ratios. It was significantly higher for SA 10% and SA 15% in the biceps, compared to CSA. In the tibials, SA 15% electrodes achieved also higher DP ratio values compared to CSA electrodes. The Ω ratio was also reduced by higher salt concentration. SA 10% showed higher values in the tibials, SA 15% showed lower values in the biceps, and SA 25% showed lower values in the biceps and quadriceps, compared to CSA electrodes.

Table 2
Indices of noise and motion artifacts.

	Biceps	Triceps	Tibials	Quadriceps
SN ratio (dB)				
CSA	37 ± 4	44 ± 9	30 ± 7	38 ± 9
SA 10%	39 ± 5*	44 ± 10	33 ± 9	36 ± 10
SA 15%	39 ± 4*	43 ± 11	32 ± 8	39 ± 9*
SA 25%	40 ± 3*	44 ± 10	30 ± 7	39 ± 9
SM ratio (dB)				
CSA	47.5 ± 16.4	62.9 ± 20.2	57.7 ± 20.4	60.5 ± 20.3
SA 10%	45.3 ± 17.2	48.3 ± 19.7*	32.8 ± 18.7*	49.1 ± 13.5*
SA 15%	50 ± 18.9	54.7 ± 17	43.6 ± 21.6*	52 ± 15.8*
SA 25%	49.3 ± 18.5	57.1 ± 16.9	44.3 ± 17.1*	53.5 ± 15.8
DP ratio (dB)				
CSA	65 ± 4	62 ± 11	52 ± 8	52 ± 6
SA 10%	67 ± 5*	65 ± 13	56 ± 8	54 ± 8
SA 15%	67 ± 5*	61 ± 12	54 ± 7*	52 ± 7
SA 25%	67 ± 4	60 ± 12	52 ± 8	50 ± 6
Ω ratio (unitless)				
CSA	1.8 ± 0.12	1.38 ± 0.07	1.51 ± 0.11	1.34 ± 0.13
SA 10%	1.77 ± 0.12	1.4 ± 0.11	1.69 ± 0.34*	1.37 ± 0.11
SA 15%	1.76 ± 0.13*	1.39 ± 0.12	1.58 ± 0.22	1.3 ± 0.09
SA 25%	1.76 ± 0.12*	1.37 ± 0.08	1.54 ± 0.19	1.29 ± 0.09*

Values are expressed as mean ± standard deviation.
CSA: Carbon/Salt/Adhesive; SA: Salt/Adhesive; SN ratio: signal-to-noise ratio; SM ratio: signal-to-motion ratio.
* means statistically significant difference ($p < 0.05$).

4. Discussion

Applications of sEMG include orthopedics, rehabilitation, and sports medicine, among others [14,15]. Given the considerable increase of knowledge about sEMG, many efforts have been carried out to improve the quality of electrodes for sEMG [16]. Several materials and various shapes and sizes have been tried over the years [16]. Ag/AgCl electrodes have become the gold standard for sEMG signal collection. We have contributed by developing dry electrodes that do not require silver and hydrogel, which might provide longer shelf life and lower cost, compared to the gold standard Ag/AgCl hydrogel electrodes.

Electrode performance is usually thought to be driven primarily by the impedance, which in CSA electrodes is a function of carbon or salt levels. However, the particular contribution of each of the different components in the adhesive layer to the impedance seems less critical than the fact that we are able to achieve a suitable performance level with fewer ingredients. Although carbon can make a contribution to lowering impedance, it does not result in improved performance, in fact, it seems to introduce unnecessary complexity (and cost) to the fabrication process. For this reason, we focused the study on the performance of SA electrodes with different levels of salt concentration.

In the present study, CSA and SA electrodes were first compared by means of impedance measurements. SA 10% electrodes presented much higher electrode-skin impedance, compared to other electrodes. This affected the performance of these electrodes in all the quality parameters. CSA, SA 15% and SA 25% electrodes showed impedance values in the same order of magnitude (a few hundred kΩ at 4 Hz) in the range of interest, 4 Hz to 2 kHz.

There are three reasons why we did not include gold standard Ag/AgCl electrodes in this evaluation study. First, given the impossibility of placing three pairs of electrodes on subjects' muscles, comparison could only be made between two types of electrodes. Second, in our previous study CSA electrodes outperformed Ag/AgCl electrodes [2]; for that reason we chose to compare SA electrodes to the best available alternative. Third, to analyze the need for carbon in the mixture, we considered the best option to compare identical electrodes, with the only difference being carbon or no carbon in the mixture (besides the varying salt concentration in the SA electrodes).

In amplitude measurements, all electrodes exhibited higher mean amplitude values during contraction, compared to the relaxation period. Nevertheless, SA electrodes tended to provide higher amplitudes than CSA in both relaxation and contraction stages. Only SA 10% amplitude mean values were lower than CSA in triceps, tibials and quadriceps (significantly lower in the latter). Considering the mean values, salt concentration increased the resulting amplitude of sEMG signals.

Overall, correlation values were very high for the linear envelopes, RMS envelopes and PSD. This means that the morphology of sEMG signals obtained using both CSA and SA electrodes were dynamically similar.

Findings based on indices of spectral analysis are more interesting. Mean values of SN ratio from SA electrodes were mostly higher compared to CSA electrodes. This suggests that adding carbon to the CSA electrode mixture introduced noise to the sEMG signals, as the Z-direction aligned carbon particles in the adhesive layer increase CSA electrodes' sensitivity to a wide range of frequencies, including higher frequencies where noise interference is present. In this aspect, SA electrodes exhibited an advantage over the CSA electrodes.

However, SM ratio from SA electrodes was in most cases significantly lower. This shows a clear advantage in adding carbon to the adhesive layer, with the corresponding activation process and a bridge layer. The better response of CSA electrodes to motion artifacts can be explained by considering the parallel multiple isolated Z direction conductive pathways in the adhesive produced by electrophoresis (activation), that are then connected through the bridge. Orientation of pathways in the Z direction reduces the effects of movement in the X and Y directions. Nevertheless, salt partially compensates for the absence of carbon, as we found increases in SM ratio when salt concentration was increased in the SA electrodes.

The computed DP ratio was significantly higher for SA 15% electrodes in biceps and tibials, compared to CSA. This suggests that SA 15% electrodes provide sEMG signals more sensitive to myographic activity, and can more reliably detect an absence of muscle activity, compared to CSA electrodes. In contrast to the SM ratio, the DP

ratio is reduced by increasing salt concentration in SA electrodes. As a result, SA 25% did not show advantages compared to CSA.

Exploring more the disadvantages of SA 10%, we also found it exhibited higher spectral deformation, measured by the Ω ratio (significant in the tibials), compared to CSA electrodes. The Ω ratio indicates the proper spectral distribution of sEMG electrodes, independent of muscle fatigue, and is also sensitive to motion artifacts. The Ω ratio suggests that SA 15% and SA 25% exhibited a more suitable spectral distribution (had lower values), compared to CSA electrodes.

Overall, inclusion of carbon enabled CSA electrodes to perform better in terms of handling motion artifacts, but the other measures (response to noise corruption (SN ratio), sensitivity to actual muscle activity (DP ratio) and appropriateness of spectral distribution (Ω ratio) favored the carbon-less (SA) electrodes.

Increasing salt concentration in the SA electrodes proved to be a trade-off. Although higher salt concentration improved performance in the presence of motion artifacts and reduced spectral deformation (Ω ratio), it also reduced the sensitivity to myoelectric signals (DP ratio).

We found that SA 10% electrodes exhibited the poorest performance and can be discarded. Although SA 15% and SA 25% electrodes exhibited similar performance, the DP ratio was higher (better) for SA 15%. It was significantly higher than that of CSA electrodes in the biceps and tibials, whereas SA 25% electrodes were not significantly different than CSA electrodes. Furthermore, SA 15% is a better option considering that lower salt concentration reduces the risk of any skin irritation.

5. Conclusion

Electrodes made without adding carbon to the adhesive, specifically a mixture with 15% salt (SA 15%) provided a better response to myoelectric activity and seem to be the most suitable alternative for sEMG data collection, compared to electrodes with carbon in the adhesive layer (CSA electrodes). Nevertheless, CSA electrodes provide a better capability to manage motion, but are more susceptible to noise corruption and are less sensitive to myoelectric activity.

Acknowledgements

The present study was supported by FLEXcon.

References

[1] I. Benedek, Pressure-sensitive Adhesives and Applications, CRC Press, 2004.
[2] H.F. Posada-Quintero, R.T. Rood, K. Burnham, J. Pennace, K.H. Chon, Assessment of Carbon/Salt/Adhesive electrodes for surface electromyography measurements, IEEE J. Transl. Eng. Health Med. 4 (2016) 1–9.
[3] H.F. Posada-Quintero, B.A. Reyes, K. Burnham, J. Pennace, K.H. Chon, Low impedance carbon adhesive electrodes with long shelf life, Ann. Biomed. Eng. 43 (2015) 2374–2382, http://dx.doi.org/10.1007/s10439-015-1282-y.
[4] H.F. Posada-Quintero, R. Rood, Y. Noh, K. Burnham, J. Pennace, K.H. Chon, Dry carbon/salt adhesive electrodes for recording electrodermal activity, Sens. Actuators Phys. 257 (2017) 84–91, http://dx.doi.org/10.1016/j.sna.2017.02.023.
[5] A. Burden, R. Bartlett, Normalisation of EMG amplitude: an evaluation and comparison of old and new methods, Med. Eng. Phys. 21 (1999) 247–257.
[6] P.W. Hodges, B.H. Bui, A comparison of computer-based methods for the determination of onset of muscle contraction using electromyography, Electroencephalogr. Clin. Neurophysiol. 101 (1996) 511–519.
[7] S. Mulroy, J. Gronley, W. Weiss, C. Newsam, J. Perry, Use of cluster analysis for gait pattern classification of patients in the early and late recovery phases following stroke, Gait Posture 18 (2003) 114–125, http://dx.doi.org/10.1016/S0966-6362(02)00165-0.
[8] H.J. Hermens, B. Freriks, R. Merletti, D. Stegeman, J. Blok, G. Rau, C. Disselhorst-Klug, G. Hägg, European recommendations for surface electromyography, Roessingh Res. Dev. 8 (1999) 13–54.
[9] C.J. De Luca, The use of surface electromyography in biomechanics, J. Appl. Biomech. 13 (1997) 135–163.
[10] A. Arvidsson, A. Grassino, L. Lindström, Automatic selection of uncontaminated electromyogram as applied to respiratory muscle fatigue, J. Appl. Physiol. 56 (1984) 568–575.
[11] C. Sinderby, L. Lindström, A.E. Grassino, Automatic assessment of electromyogram quality, J. Appl. Physiol. Bethesda Md 79 (1995) (1985) 1803–1815.
[12] A.D. Chan, G.C. Green, Myoelectric control development toolbox, Proc. 30th Conf. Can. Med. Biol. Eng. Soc. (2007) M0100–M0101, http://www.sce.carleton.ca/faculty/chan/matlab/matlab_library_old/myoelectric%20control%20development%20toolbox.pdf (Accessed 14 December 2015).
[13] P. McCool, G.D. Fraser, A.D.C. Chan, L. Petropoulakis, J.J. Soraghan, Identification of contaminant type in surface electromyography (EMG) signals, IEEE Trans. Neural Syst. Rehabil. Eng. Publ. IEEE Eng. Med. Biol. Soc. 22 (2014) 774–783, http://dx.doi.org/10.1109/TNSRE.2014.2299573.
[14] G.D. Meekins, Y. So, D. Quan, American Association of Neuromuscular & Electrodiagnostic Medicine evidenced-based review: use of surface electromyography in the diagnosis and study of neuromuscular disorders, Muscle Nerve 38 (2008) 1219–1224, http://dx.doi.org/10.1002/mus.21055.
[15] G. Drost, D.F. Stegeman, B.G.M. van Engelen, M.J. Zwarts, Clinical applications of high-density surface EMG: A systematic review, J. Electromyogr. Kinesiol. 16 (2006) 586–602, http://dx.doi.org/10.1016/j.jelekin.2006.09.005.
[16] H.J. Hermens, B. Freriks, C. Disselhorst-Klug, G. Rau, Development of recommendations for SEMG sensors and sensor placement procedures, J. Electromyogr. Kinesiol. 10 (2000) 361–374, http://dx.doi.org/10.1016/S1050-6411(00)00027-4.

Biographies

Hugo F. Posada-Quintero received his B.S degree in electronic engineering from the Universidad Distrital Francisco José de Caldas in Bogotá D.C., Colombia, M.S. degree in electronics and computers engineering from Universidad de los Andes, Bogotá D.C., Colombia, and Ph.D. in biomedical engineering from the University of Connecticut, Storrs. Currently, he is a postdoctoral researcher in the biomedical engineering department at the University of Connecticut. His topics of interest are mainly biomedical signal processing and biomedical instrumentation.

Ryan T Rood received the B.S degree in biomedical engineering from the University of Connecticut, 2015 with a minor in electronics and systems. Currently, he is pursuing a M.S degree in biomedical engineering at the University of Connecticut. His topic of interest is biomedical instrumentation.

Ken Burnham has over 32 years experience performing product and process development in R&D for major manufacturing companies. His areas of expertise include mechanical & electrical engineering technology. Ken holds an A.S. in Mechanical Engineering Technology from Springfield Technical Community College in Springfield MA and has many patents granted worldwide. He is currently Engineering Technologist at FLEXcon Co. in Spencer MA. Prior to joining FLEXcon, Ken spent 13 years working for Proctor and Gamble.

John Pennace is an executive of FLEXcon Company, Inc. He obtained his B.S. degree in Chemistry at Lowell Technological Institute ('69), M.S. degree in Chemistry at Tufts University ('72), and MBA at Babson College ('80). He is the Manager New Ventures.

Ki H. Chon received the B.S. degree in electrical engineering from the University of Connecticut, Storrs; the M.S. degree in biomedical engineering from the University of Iowa, Iowa City; and the M.S. degree in electrical engineering and the Ph.D. degree in biomedical engineering from the University of Southern California, Los Angeles. He spent three years as an NIH Post-Doctoral fellow at the Harvard-MIT Division of Health Science and Technology. He is currently the John and Donna Krenicki Chair Professor and Head of Biomedical Engineering at University of Connecticut, Storrs, CT.